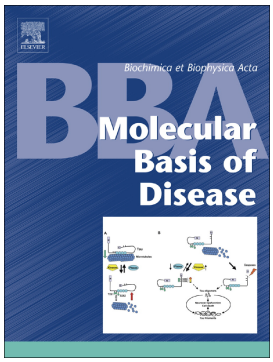

Matrix stiffness modulates ILK-mediated YAP activation to control the drug resistance of breast cancer cells

Xiang Qin, Xiaoying Lv, Ping Li, Rui Yang, Qiong Xia, Yu Chen, Yueting Peng, Li Li, Shun Li, Tingting Li, Ying Jiang, Hong Yang, Chunhui Wu, Chuan Zheng, Jie Zhu, Fengming You, Heng Wang, Jiong Chen, Yiyao Liu

PII: S0925-4439(19)30353-9

DOI: https://doi.org/10.1016/j.bbadis.2019.165625

Reference: BBADIS 165625

To appear in: *BBA - Molecular Basis of Disease*

Received date: 13 June 2019

Revised date: 7 November 2019

Accepted date: 26 November 2019

Please cite this article as: X. Qin, X. Lv, P. Li, et al., Matrix stiffness modulates ILK-mediated YAP activation to control the drug resistance of breast cancer cells, *BBA - Molecular Basis of Disease*(2019), https://doi.org/10.1016/j.bbadis.2019.165625

Matrix stiffness modulates ILK-mediated YAP activation to control the drug resistance of breast cancer cells

Xiang Qin [1,3], Xiaoying Lv [1], Ping Li [1], Rui Yang [1], Qiong Xia [1], Yu Chen [1], Yueting Peng [1], Li Li [1,3], Shun Li [1,3], Tingting Li [1,3], Ying Jiang [1,3], Hong Yang [1,3], Chunhui Wu [1,3], Chuan Zheng [2], Jie Zhu [2], Fengming You [2], Heng Wang [4], Jiong Chen [4], Yiyao Liu [1,2,3 *]

[1] Department of Biophysics, School of Life Science and Technology, University of Electronic Science and Technology of China, Chengdu 610054, Sichuan, P.R. China; [2] Hospital of Chengdu University of Traditional Chinese Medicine, No. 39 Shi-er-qiao Road, Chengdu 610072, Sichuan, P.R. China; [3] Center for Information in Biology, University of Electronic Science and Technology of China, Chengdu 610054, Sichuan, P.R. China; [4] State Key Laboratory of Pharmaceutical Biotechnology and MOE Key Laboratory of Model Animals for Disease Study, Model Animal Research Center, Nanjing University, Nanjing 210061, Jiangsu, P.R. China

[*] To whom correspondence should be addressed:

Prof. Yiyao Liu, Ph.D

School of Life Science and Technology, University of Electronic Science and Technology of China, and Hospital of Chengdu University of Traditional Chinese Medicine, Chengdu, Sichuan, P. R. China. Tel: +86-28-8320-3353, fax: +86-28-8320-8238, E-mail: liuyiyao@uestc.edu.cn

Abstract

One of the hallmarks of cancer progression is strong drug resistance during clinical treatments. The tumor microenvironment is closely associated with multidrug resistance, the optimization of tumor microenvironments may have a strong therapeutic effect. In this study, we configured polyacrylamide hydrogels of varying stiffness [low (10 kPa), intermediate (38 kPa) and high (57 kPa)] to simulate tissue physical matrix stiffness across different stages of breast cancer. After treatment with doxorubicin, cell survival rates on intermediate stiffness substrate are significantly higher. We find that high expression of ILK and YAP reduce the survival rates of breast cancer patients. Drug resistance is closely associated with the inactivation of the hippo pathway protein Merlin/MST/LATS and the activation of YAP. These results not only highlight the understanding of drug resistance mechanisms but also serve as a new basis for developing breast cancer treatment delivery systems.

Key words: Matrix stiffness; ILK; YAP; Drug resistance; Mechanotransduction

Abbreviations

ECM: Extracellular matrix; ILK: Integrin-Linked Kinase; YAP/TAZ: Yes-Associated Protein/ Transcriptional coactivator with PDZ-binding motif; DOX: Doxorubicin; MST: Macrophage-stimulating; LATS: Large tumor suppressor; ILKAP: Integrin-linked kinase-associated serine/threonine phosphatase; PINCH1: Particularly interesting new cysteine-histidine-rich protein; PARP: Poly ADP-ribose polymerase; ABC: ATP-binding cassette; ANKRD: Ankyrin repeat domain; CTGF: Connective tissue growth factor; CYR61: Cysteine-rich angiogenic inducer 61; ATCC: American Type Culture Collection; PAA gel: Polyacrylamide hydrogel; APS: Ammonium persulfate; TEMED: Tetramethylethylenediamine; CCK-8: Cell counting kit-8; PI: Propidium iodide; PBS: Phosphate buffer saline; BSA: Bovine serum albumin; ECL: Electrogenerated chemiluminescence; P-gp: P-glycoprotein; HRP: Horseradish peroxidase.

1. Introduction

Breast cancer is a disease caused by multiple forms of mammary gland dysplasia, which is highly heterogeneous [1]. Chemotherapy is currently one of the ways for treatments, but patients are prone to drug resistance [2]. Therefore, determining the mechanisms of drug resistance and the optimization of treatment plans for breast cancer patients are urgent problems to be solved in clinical practice. The formation and development of tumor cells are closely related to the tumor microenvironment, which can provide the necessary material basis for tumor invasion, metastasis and drug resistance [3-7]. Interactions between cells and microenvironments are regulated by the extracellular matrix (ECM). Physical ECM properties (e.g., spatial arrangement, pore size, matrix stiffness and insolubility) not only ensure the integrity of tissues but also regulate cell responses to the microenvironment. The ECM is

dynamic, from production and cross-linking to degradation and remodeling. When an abnormality forms, this is often accompanied by the onset of disease such as cancer and tissue fibrosis. Solid tumor development is often accompanied by abnormal cross-linking, remodeling and the increased ECM tissue stiffness [8]. Therefore, tumor tissue stiffness can be used to facilitate the diagnosis of tumors clinically. ECM abnormalities directly leads to the malignant cell transformation and metastasis, they can also transform mesenchymal cells in the microenvironment and produce a large number of matrix degrading enzymes, chemokines and growth factors, forming a new microenvironment [9].

Research of the physiological processes of tissues has focused on biochemical signals occurring during physiological processes such as changes in molecular structures or signaling pathways, showing that the mechanical properties of cells or tissues are byproducts of their functions [10,11]. However, many organ dysfunctions and diseases can be understood as being caused by changes in the tissue mechanical properties. For example, atherosclerosis is often characterized by an increase in the stiffness of vessel walls. With age, the vascular wall matrix and cell compositions change, increasing the rigidity of the vessel wall. Under pathological conditions, due to the proliferation of mesenchymal stem cells and migration from the media to the intima, large volumes of collagen and extracellular matrix are secreted, increasing the rigidity of the vessel wall [12]. Other diseases associated with tissue mechanic dysfunction, including scleroderma caused by collagen deposition, indicate that the mechanical properties of the matrix microenvironment are closely related to disease orientation. The most aggressive triple-negative breast cancer has the highest sub-population of cancer stem cell (CSC) among different cell types [13], and the tissue stiffness with cancer progression could be an intrinsic response by the CSC to optimize cancer cell growth. Reports also showed the biphasic relation between CSC markers and matrix stiffness

[14]. Meanwhile, colorectal carcinoma cells exhibit metastatic behavior in 20-50 kPa stiffness range [15], Osteosarcoma cells interact with 55 kPa substrates optimally [16]. We used PAA gels with a Young's modulus of 10 kPa to mimic normal breast tissue or benign breast tumors and 38 kPa to mimic malignant breast tumors, 57 kPa was used to simulate the advanced stages of breast tumors that are more rigid than any breast tissue and close to bone matrix stiffness [14-17].

Integrin-Linked Kinase (ILK) is a serine/threonine kinase that acts as a key regulator of the Integrin/PI3K signaling pathway [18]. ILK is located at the site where actin is linked to integrin. It interacts with the intracellular segment of the integrin subunit and anchors itself to integrins. ILK is involved in cell migration, proliferation and apoptosis [19,20]. Hausmann *et al* found that ILK can regulate the radiation resistance of cells by interacting with ILKAP and PINCH1 [21]. However, the expression levels of ILK are inconsistent at different stiffness levels. Therefore, exploring whether matrix stiffness can affect the drug resistance of breast cancer cells through ILK is critical. YAP (Yes-Associated Protein) and TAZ (PDZ-binding motif) transcriptional coactivator have transcriptional coactivation activity, they regulate the transcriptional process of target genes [22]. Kim *et al.* confirmed that melanoma cells can promote the activation of YAP/TAZ through the remodeling of actin, a diluent promoting cell resistance to BRAF inhibitors [23]. Other researchers have shown that microenvironmental stiffness can regulate cell resistance to lapatinib through YAP/TAZ [24]. YAP/TAZ is also related to a variety of signaling molecules, the most classic being the Hippo pathway components Merlin, MST and LATS. Nonphosphorylation of the Merlin protein is its active form, which is capable of phosphorylating MST1/LATS. Phosphorylated MST1/LATS is an active form that could inactivate YAP by phosphorylation, leading to more YAP being retained in the cytoplasm, binds to 14-3-3 proteins and the initiates ubiquitination degradation pathway.

In addition to accelerating tumor development, an increase in tumor tissue stiffness can also affect drug resistance and render treatments more difficult. At present, the research on drug resistance caused by the extracellular matrix mainly focuses on two areas. The first focus is altering the diffusion of drugs and rates at where drugs pass in and out of cells. The penetration of antitumor drugs into tumor tissues with high collagen content levels (high stiffness) occurs more slowly than low collagen levels (low stiffness) [25,26]. The second collection of studies focus is on reducing cell sensitivity to drugs (e.g., by limiting cell apoptosis) [27], although specific signaling molecular mechanisms remain unknown. P-glycoprotein (P-gp) is an energy-dependent drug pump, it can reverse the concentration of drugs to pump out the drugs, which reduces the accumulation of chemotherapeutic drugs in cells, leading to drug resistance. Doxorubicin is a kind of antitumor antibiotic, which can inhibit the synthesis of RNA and DNA. It has a wide antitumor spectrum and has effects on many kinds of tumors. It is a periodic non-specific drug and has killing effects on tumour cells in various growth cycles. To study the regulations of matrix stiffness to the drug resistance, we used polyacrylamide hydrogel to simulate the different stiffness of breast cancer cells (10 kPa, 38 kPa and 57 kPa) to respectively simulate benign (fibrous tumor), malignant, and tissue stiffness during bone metastasis. It is helpful to understand the relationship between matrix stiffness and cell drug resistance as well as potential regulatory mechanisms to further guide cancer drug resistance research and disease treatments.

2. Materials and Methods

2.1 Antibodies and reagents

Cell culture medium of L15, penicillin, streptomycin and newborn calf serum (NCS) was purchased from Gibco (Grand Island, NY, USA). Polyclonal

antibodies against Ki67 were purchased from Abcam (Cambridge, UK), and Phospho-Merlin (Ser518) was purchased from Cell Signaling Technology (Beverly, MA, USA). Monoclonal antibodies against caspase-3, C-caspase-3, PARP, C-PARP, Bcl-2, Bax, β-actin, P-gp, Akt, Phospho-Akt (Ser473), LATS1, Phospho-LATS1 (Thr1079), Phospho-YAP (Ser127), and Histone 3 were purchased from Cell Signaling Technology (Beverly, MA, USA). Integrin linked kinase (ILK), Merlin, MST-1, and Phospho-MST1/2 (T180+T183) were purchased from Abcam (Cambridge, UK). YAP was purchased from Santa Cruz Technology (Santa Cruz, USA). Calcein-AM/PI and Lipofectamine LTX were purchased from Thermo Fisher Scientific (Waltham, MA, USA). Elacridar was purchased from Selleckchem (Houston, TX, USA). DAPI and Rhodamine123 were purchased from Sigma-Aldrich (St. Louis, MO, USA). T315 and verteporfin were purchased from MedChemExpress (Monmouth Junction, NJ, USA). All other reagents were used as received without additional purification unless otherwise noted.

2.2 Cell culture

The triple negative human breast cancer cell MDA-MB-231 was obtained from the American Type Culture Collection (ATCC, Manassas, VA, USA). Cells were cultured in L15 medium composed of 10% newborn calf serum and 1% penicillin and streptomycin. For culturing, we used a 37°C humidified incubator.

2.3 Preparation of polyacrylamide hydrogel

We prepared polyacrylamide hydrogel (PAA gel) involved the free radical gelation reaction of acrylamide and methylene bisacrylamide under the catalysis of ammonium persulfate (APS) and tetramethylethylenediamine (TEMED). We used low (10 kPa), intermediate (38 kPa) and high (57 kPa) PAA gel samples to simulate tissue physical matrix stiffness in different stages of breast cancer (**Supplementary Fig. S1)** [28]. For gels of each stiffness level,

the composition of 10 mL of PAA gel is shown in **Supplementary Table 1**.

2.4 Cell proliferation and death assay

Cells were reseeded in 96-well plates at 5,000 cells/well, and cell proliferation was determined using a cell counting kit-8 assay kit (CCK-8) (Dojindo, Kumamoto, Japan). In brief, cells were pretreated on different stiffness and then 20 μL of CCK-8 solution was added to the medium, followed by further incubation for 1 h. The absorbance at 450 nm was measured by spectrophotometry (BioTek, VT, USA). To quantify the number of live and dead cells, cells were costained with Calcein-AM and propidium iodide (PI). The cells were incubated in a PBS solution of Calcein-AM (2 μM) and PI (4 μM) in the dark for 20 min at room temperature. After washing, the cells were resuspended in PBS and then imaged with a fluorescence confocal microscope (FV1000, Olympus, Japan).

2.5 Immunofluorescence staining

Cells of $5X10^4$ were seeded on the substrates, fixation was followed with 4% paraformaldehyde in phosphate buffer saline (PBS) for 15 min at room temperature and blocked with 1% BSA in PBST (1×PBS, 0.1% Tween-20) for 1 h after its confluence. Cells were incubated with the indicated primary antibody overnight at 4°C and stained with Alexa-conjugated secondary antibodies for 1 h at room temperature. After being rinsed 3 times in PBST for 5 min, the samples were visualized on a confocal laser scanning microscope (FV1000, Olympus, Japan). The fluorescence intensity and colocalization calculations of the confocal images were analyzed by using Image J software (NIH, USA), the intensity in certain regions were selected and the mean values were recorded. Each image was 16-bit and Image J Plugin deconvolution was performed before the analysis.

2.6 Flow cytometry

To analyze the cell doxorubicin intake and efflux, cells on varying stiffness were collected, rinsed with rinsing buffer (1×PBS, 2 mM EDTA, 0.5% BSA), resuspended in 4% paraformaldehyde for 15 min at 4°C, rinsed 3 times in PBS and resuspended at 1×10^6 cells/mL in rinsing buffer. The cells were incubated at 4°C for 1 h and then rinsed 3 more times in rinsing buffer, and the mean fluorescence intensities were measured using a flow cytometer (FACSCalibur, BD, USA).

2.7 Reverse transcription-PCR (RT-PCR) and quantitative PCR (qPCR)

Total cell RNA was extracted using the RNAiso Plus kit (Takara, Shiga, Japan) and reverse transcribed using the PrimeScriptTM RT reagent kit (Takara). The real time-PCR analysis was performed in accordance with the manufacturer's instructions using SYBR Premix Ex Taq II (Tli RNaseH Plus) (Takara). The master mix contained Takara Ex Taq HS, dNTP mixture, Mg^{2+}, Tli RNaseH and SYBR Green I. One microliter of reverse transcription reaction was used for a total 10-μL quantitative PCR reaction. Relative mRNA levels of each gene were analyzed following the comparative C_t method. Data are presented as fold-changes. The primers used are listed in **Supplementary Table 2**.

2.8 Western blot analysis

Protein isolation was carried out using cell lysis buffer (50 mM NaF, 10 mM $Na_2P_2O_7$, 2%SDS, 1 mM) supplemented with protease inhibitor cocktail (Roche, South San Francisco, CA, USA) and phosphatase inhibitor cocktails I and II (Sigma-Aldrich, Saint Louis, MO, USA). Following electrophoretic separation by 10% SDS-polyacrylamide gel electrophoresis, proteins were electroblotted onto polyvinylidene fluoride membranes (Millipore, Billerica, MA, USA). The membranes were then blocked with Tris-buffered saline containing 0.1% Tween-20 (TBST) and 5% bovine serum albumin for 1 h at room temperature. For extraction of nuclear and cytoplasmic proteins, nuclear

extraction kit (Solarbio, China) was used for collecting the nucleus before lysis. Antibodies against C-caspase-3, caspase-3, C-PARP, PARP, Bcl-2, Bax, P-gp, ILK, p-Akt, Akt, p-Merlin, Merlin, p-MST1, MST, p-LATS1, LATS1, p-YAP, YAP, Histone 3 and β-actin were used according to the manufacturer's instructions. Incubation was performed overnight at 4°C with light shaking. Thereafter, membranes were rinsed with TBST buffer, and further incubation was carried out with an HRP-conjugated antibody for 1 h at room temperature. For the visualization of protein bands, an enhanced electrogenerated chemiluminescence (ECL) system (Amersham, Chicago, IL, USA) was used. Evaluation of the bands was performed by densitometric analysis. The protein level expression of cytoplasm was determined by normalizing to that of the housekeeping protein β-actin, while nucleus expression was determined by normalizing to Histone 3.

2.9 Dual-luciferase reporter assay

For the measurement of reporter activity, the 36 kD-luciferase reporter plasmid and pRL-TK were cotransfected into MDA-MB-231 cells. Luciferase activity was measured using a dual luciferase reporter assay system (Beyotime, China) according to the manufacturer's instructions and detected by a Fluoroskan Ascent FL (Thermo) 48 h after the transfections. Luciferase activity levels were normalized for Renilla luciferase activity. All conditions were tested in triplicate wells.

2.10 Kaplan-Meier survival analysis

The microarray expression profile was collected from the Oncomine public sample database (http://www.oncomine.org). As fitting targets, we studied patients with normal breast or breast cancer who were analyzed in terms of ILK and YAP expression. All the selected data were analyzed based on the R_2 microarray public database (http://r2.amc.nl) or GraphPad Prism Software version 6.0.

2.11 Statistical analysis

To eliminate errors, each experiment was repeated at least three times. Data were collected as means ± SDs. A t-test was used to analyze the data with two distribution tails. A value of $p<0.05$ was used to determine statistically significant differences, and values of $p<0.005$ and $p<0.0005$ were considered to be remarkably statistically significant. The p-value derived from the Kaplan-Meier survival analysis was calculated through a log-rank test. The results were analyzed with GraphPad Prism software 6.0.

3. Results

3.1 Intermediate rigidities promoted the survival rates of breast cancer cells

The proliferation of tumor cells is closely related to the growth, metastasis and recurrence of tumors. Cell death represents an important phase of normal organism development [29], the steady state between cell proliferation and death is critical for maintaining normal physiological processes. We thus investigated the survival rates of MDA-MB-231 cells on matrix of varying stiffness after doxorubicin treatment. Doxorubicin is an antineoplastic and cytotoxic drug that acts on the chemical structure of DNA and RNA. It can kill tumor cells in various growth cycles and also affect normal cells. Therefore, the most used concentration is generally 2-5 mg/L. In this study, the killing effects of Doxorubicin on cancer cells in different stiffness were verified by this experiment, and the concentration of 3 mg/L was selected for the subsequent experiments. Under this concentration, the cell survival rates at 10/38/57 kPa were all higher than 70%, the results were shown in Fig. 1A. Further, the expression of Ki67 was measured by immunofluorescence, and it can be observed that the expression of Ki67 in cells on low and high stiffness substrates were significantly lower than intermediate stiffness substrate (**Fig. 1B** and **C)**. The above results confirmed that the proliferations of cells on low and high stiffness substrates after doxorubicin treatments were significantly

lessened. Calcein-AM/PI co-staining shown in **Fig. 1D** and **E** revealed that the number of red cells on low and high stiffness substrates was significantly greater than the number observed on the intermediate stiffness substrate, showing that there were more dead cells on low and high stiffness substrates (Cell death rates at 10 kPa, 38 kPa and 57 kPa were 48.5%, 29.6% and 55.2%, respectively). We also quantified the expression of apoptosis-related proteins on varying stiffness after doxorubicin treatment by Western blot. **Fig. 1F** and **G** illustrated the increased expression of cleaved Caspase-3 and PARP and the decreased expression of Bcl-2 in low and high stiffness substrates, thus depicting activation of the apoptotic pathway. These results indicated that cells on low and high stiffness substrates were more sensitive to doxorubicin.

3.2 Intermediate stiffness matrix decreased doxorubicin uptake of breast cancer cells

Doxorubicin, as a topoisomerase II inhibitor, is widely used in the clinical treatment of breast cancer [30]. As a reduction in drug intake in cells promotes drug resistance, we explored the uptake of doxorubicin by cells at different stiffness levels. As is shown in **Fig. 2A**, cell fluorescence intensities observed from low and high stiffness substrates were significantly higher than intermediate stiffness substrate, which indicated lower intracellular doses of doxorubicin. We further verified the results by flow cytometry. The results showed peaks of intermediate stiffness substrate to the left, meaning that the fluorescence intensity of the 38 kPa group was lower than that of the other two groups (**Fig. 2B** and **C**). The above results indicated that compared to low and high stiffness substrates, cells on intermediate stiffness substrate can significantly reduce the uptake of doxorubicin.

3.3 Intermediate stiffness matrix induced doxorubicin efflux via P-gp in breast cancer cells

As the ATP-binding cassette (ABC) transporter family can limit the accumulation of drugs by promoting drug efflux [31], we explored rhodamine (rho123) efflux to observe the efflux of cellular drugs at different stiffness levels. Rhodamine was used as a fluorescent substrate for P-gp, and Elacridar was used as an inhibitor of P-gp. The flow cytometry results were shown in **Fig. 2D**, and the fact that the peak to the right indicated that fluorescence levels of Rho123 in the cell were strong, meaning that the levels of extracellular efflux were low. The peak of the Elacridar group was located to the far right because Elacridar inhibited the activity of P-gp and thus limited the transport of P-gp to Rho123. This was followed by the low, high and intermediate stiffness substrates. The average fluorescence intensity of the Elacridar group was found to be the highest, while that of the intermediate stiffness substrate was found to be the lowest. This means that the external efflux of the intermediate stiffness substrate group was more pronounced than the low and high stiffness substrates groups. The results also indicated that the expression of P-gp at the mRNA and protein levels were more pronounced on intermediate stiffness substrate (**Fig. 2E** and **F**). In summary, matrix stiffness levels can affect cell drug resistance via P-gp.

3.4 Matrix stiffness affected breast cancer cell ILK expression

ILK acts as a sensor of tissue mechanics and as a hypoxic microenvironment that regulates the characteristics of breast cancer stem-like cells. Therefore, we explored whether ILK was involved in stiffness-dependent cell drug resistance. We first used the Oncomine public sample database (www.oncomine.org) to analyze the expression of ILK mRNA levels in 144 breast tissue samples and 90 breast cancer tissue samples. The results were shown in the left panel of **Fig. 3A**. The expression of ILK in breast carcinoma was significantly higher than that in breast tissue. We also analyzed the expression of ILK in different stages of breast cancer (stage I-IV). As is shown

in the right panel of **Fig. 3A**, with breast cancer progression, the expression of ILK in stage IV was significant higher than stage I. We also used the R_2 database to analyze the survival rates of breast cancer patients with different ILK expression. From **Fig. 3B**, we found that the survival rate of patients with high ILK expression was lower than that of patients with low ILK expression. This indicated that in the development of breast cancer, expression levels of ILK change will affect the patient survival rate. The results of ILK expression at the mRNA and protein levels at different stiffnesses were varied (**Fig. 3C-E**). ILK mRNA and protein levels were significantly lower in low and high stiffness substrates than on intermediate stiffness substrates for both MDA-MB-231 and MDA-MB-468 cells. This showed that matrix stiffness affected ILK expression.

3.5 ILK increased breast cancer cell drug resistance

It has been demonstrated that ILK expression on an intermediate rigidity is more pronounced than on low and high stiffness substrates. We examined whether the matrix stiffness of breast cancer cells can affect the cell resistance process via ILK. To identify our hypothesis, we selected ILK inhibitor T315 to observe drug resistance effects [32]. T315 is a small molecule inhibitor that effectively promotes the dephosphorylation of AKT at Ser-473 and the dephosphorylation of other related ILK targets. We examined the phosphorylation of Akt in MDA-MB-231, MDA-MB-468, and BT-549 cells treated with different concentrations of T315 for 48 h. It can be observed that when the concentration of T315 reached 2 μM, the phosphorylation of Akt was significantly inhibited (**Fig. S2**). Cell death was observed by Calcein-AM/PI costaining. As the concentration of T315 increased, the cell death rate increased to 86.7% (**Fig. S2**), indicating that the inhibition of ILK can promote cell sensitivity to doxorubicin. Further results showed no difference in IC_{50} values at different stiffness levels after treatment with T315 for MDA-MB-231 or MDA-MB-468. This suggests that the inhibition of ILK can eliminate

stiffness-dependent drug resistance.

3.6 Intermediate rigidity induced YAP-mediated P-gp expressions

In relation to the stiffness-dependent drug resistance of breast cancer cells, we examined whether stiffness can affect YAP translocations, ultimately regulating breast cancer cell drug resistance. To confirm this hypothesis, we analyzed the survival rates of patients with different expression levels of YAP based on the R_2 database. It was found that survival rates of patients with high levels of YAP expression were lower (**Fig. 4A**). We used Western blot to measure the expression of YAP and its upstream molecules. **Fig. 4B** shows that p-Merlin expression on an intermediate stiffness substrate was more pronounced than low and high substrates, while p-MST1 and p-LATS1 expression levels were relative low. For both low and high rigidities, the expression of p-YAP is higher than intermediate stiffness substrate. These results showed that the activation of YAP (De-phosphorylation status of YAP) on an intermediate stiffness substrate was stronger than other substrates. We further performed a luciferase reporter gene assay to determine the transcriptional activity of YAP target genes (ANKRD1, CTGF and CYR6), which were found to be more active on the intermediate rigidity (**Figs. 4C-E**). To determine whether the difference in YAP transcriptional activity observed was associated with P-gp and responsible for drug resistance, we used the YAP inhibitor Verteporfin and ILK inhibitor T315 to treat the cells. The expression of P-gp mRNA declined with increasing verteporfin concentration on intermediate stiffness substrate. T315 also significantly reduced P-gp expressions. This showed that the inhibition of YAP and ILK can reduce the expression of the drug resistance gene P-gp expressions, thereby regulating the drug resistance of breast cancer cells.

3.7 ILK mediated intermediate stiffness matrix YAP activation

We found that matrix stiffness can affect ILK expression and YAP

translocation, while YAP acts as a transcription factor and activates downstream target gene expression. Therefore, we examined whether ILK can act as an intermediate molecule during YAP matrix stiffness regulation. We used the Oncomine public sample database to explore the correlation between ILK and YAP in terms of mRNA expression. As is shown in **Fig. 5A**, there was a significantly positive correlation between ILK and YAP mRNA expression in both normal breast tissue (left panel) and breast carcinoma tissue (right panel). Since the previous results have shown that ILK was highest at 38 kPa, we therefore treated cells on intermediate stiffness substrate with the ILK inhibitor T315. We quantitatively analyzed the fluorescence intensity in the cytoplasm and nucleus and determined whether YAP was redistributed in the cytoplasm or nucleus according to the ratio of fluorescence intensity. As the concentration of T315 increased, YAP nuclear translocation reduction was observed, showing that YAP activity was regulated by ILK. Western blot also showed that after inhibition of ILK, p-YAP, p-MST1 and p-LATS1 expression increased, while p-Merlin expression decreased. This showed that the inhibition of ILK can prevent the activation of YAP (**Figs. 5B-D**). These results demonstrated that the transcriptional activity of YAP was stronger on intermediate stiffness substrate.

3.8 Intermediate stiffness matrix induced YAP expression and activity

The YAP fluorescence intensity observed in the nucleus of an intermediate stiffness substrate was found to be significantly stronger than that in the cytoplasm, and this phenomenon was not obvious for low and high stiffness substrates (**Fig. 6A** and **B**). It can be observed that with regard to stiffness levels, more YAP was translocated into the nucleus of cells on the intermediate rigidity. We further extracted cytoplasmic and nuclear proteins of MDA-MB-231 cells of varying stiffness. Corresponding results were shown in Fig. 6C, p-YAP expression in the cytoplasm of an intermediate stiffness substrate was

observed to be less pronounced than that of low and high stiffness substrates, while YAP levels in the nucleus on intermediate stiffness substrates were significantly higher than low and high stiffness substrates. These results confirmed that the activation of YAP matrix plays a positive role to strong drug resistance.

4. Discussion

The effects to tumor ECM stiffness are multifaceted, involving the regulation of tumor proliferation, apoptosis, and migration. In the treatment of cancer, cells will gradually develop drug resistance, which is an important factor in the poor prognosis of cancer patients. At present, research on drug resistance mainly focuses on drug inactivation, drug target changes, drug efflux, DNA damage repair, and apoptosis inhibition. However, research on the relationship between matrix stiffness and drug resistance is rare. We focused on breast cancer cells by configuring polyacrylamide hydrogels of varying stiffness to simulate the tissue characteristics of breast cancer of different stages, and we found that cell proliferation on intermediate stiffness substrate was significantly stronger than observed on low and high stiffness substrates, while the proportion of dead cells was significantly reduced. Matrix stiffness regulated the uptake and efflux of cells to cell drug resistance. Matrix stiffness can also affect cell contractility (cytoskeleton) and enzymes that associated with cell growth and differentiation (e.g., Rho, ERK, etc.) [33]. Matrix stiffness regulated the conversion of a normal phenotype to a malignant phenotype by regulating the activation and expression of integrins [34]. This microenvironmental change has been thought to contribute to the development and progression of cancer.

An increase in tumor tissue stiffness affects drug resistance and renders treatments more difficult. We have demonstrated that different stiffness levels can trigger differences in drug resistance properties. We explored the related

molecular mechanisms and identified molecular pathways that can transmit mechanical signals of stiffness levels to cells, thereby changing the response of cells to drugs. Studies have shown that ILK can act as a sensor of tissue mechanics and as a hypoxic microenvironment to regulate the characteristics of breast cancer stem-like cells [35]. YAP can also act as a mechanical sensor molecule in cells, responding to changes in a variety of extracellular mechanical states [36]. Moreover, ILK and YAP can regulate cell resistance by participating in multiple signaling pathways [23,37]. Our study showed that ILK expression varies at different stiffness levels, with the highest levels of ILK expression observed from intermediate stiffness substrates. After inhibiting ILK, cell resistance decreased, indicating that ILK can promote cell tolerance to doxorubicin and that matrix stiffness can affect cell resistance by regulating ILK expression. However, whether ILK is the only molecule that binds to integrin on the cell membrane and its specific mechanism of resistance require further investigations. YAP/TAZ, a co-transcriptional activator, is involved in the development of drug resistance. In relation to resistance-dependent cell resistance, whether YAP/TAZ participates in this process and the relationship between ILK and YAP were explored. The results confirmed that YAP can promote cell drug resistance. ILK can mediate YAP activity and nuclear translocation to regulate stiffness-dependent drug resistance. This study explored the molecular mechanisms involved in ILK and identified molecular pathways that can transmit mechanical signals of stiffness to cells, thereby changing cell responses to drugs. The role of YAP during mechanotransduction is not universal, the lack of YAP activity in 3D culture shows an independent manner [38]. It indicates that role of YAP might be different in different tumor microenvironments.

As cells produce more tension on hard substrates [39], cells tend to spread on harder substrates in 2D. Within a certain range, as the stiffness increases, the spreading area of the cancer cells and the growth rate of the

circumference are faster. As the stiffness level continues to increase, the spread area and circumference growth rate decrease [40]. In addition to affecting cell area and circumference, matrix stiffness shortens the period of cell spread [41]. In stem cells, cell stress fibers on a medium-stiffness substrate are positioned parallel to the long axes of cells [42]. Matrix stiffness levels may regulate cell motility by affecting cell spread and cytoskeletal alignment. As ILK exists at the junction between actin and integrin, there might be a correlation between the cytoskeleton and drug resistance, which requires more in-depth investigation.

The increase in tumor stiffness that occurs mainly results from the deposition of type I collagen fibers. During tumor growth, collagen is fibrotic and forms a tight bundle. It has been suggested that imaging or minimally invasive biopsies can be used clinically to measure collagen recombination [43], which can be used to determine the risk of tumor metastasis or patient prognosis. In fact, mammography and palpation tools are often used to clinically identify dense breast tissue as a routine indicator for breast cancer diagnosis. Therefore, stiffness is an indicator of the tumor microenvironment. The high resistance of intermediate stiffness substrate microenvironment that observed in this study was achieved by ILK-mediated YAP activation. Merlin, MST1, and LATS1 are mainly involved in the activation of YAP. Our study offers a theoretical foundation for elucidating the mechanism of cancer orientation and development. Our work also presents ideas on the diagnosis and treatments of clinical tumors from the perspective of drug selection.

In summary, ILK expression on intermediate stiffness substrate is greater than that observed on low and high stiffness substrates, and inhibition of ILK leads to a decline in cell drug resistance. YAP translocation, dephosphorylating and high transcriptional activity on intermediate stiffness substrate were found to be more pronounced than low and high stiffness substrates. YAP inhibition desensitizes cells to drugs and decreases P-gp expression. These results

show that matrix stiffness can transmit a mechanical signal to the intracellular phase through ILK-mediated YAP activation, thereby regulating cell drug resistance (Fig.7).

Declaration of Competing Interest

The authors declare no potential conflicts of interest

Acknowledgements

This work was supported, in part or in whole, by the grants from the National Natural Science Foundation of China (11772088, 31700811, 11802056, 31800780, 11972111, 31900940, and 81671821), the China Postdoctoral Science Foundation (2018M640904, 2019T120831), the Basic Research Program of Sichuan Science and Technology Foundation (2017JY0019, 2017JY0217, 2019YJ0183, 2019YJ0184), and the Fundamental Research Funds for the Central Universities (ZYGX2019J117).

Authors' contributions

X.Q. and X.L. performed image acquisition and western blot analysis. P.L., R.Y., Q.X., Y.C. and Y.P. processed and analyzed images. L.L., S.L., T.L., Y.J., H.Y., C.W. and F.Y. did the survival rate analysis. C.Z. and J.Z. conducted the data analysis of q-PCR experiments. H.W., J.C. and X.Q. organized data. X.Q., H.W. and J.C prepared the manuscript. X.Q., X.L. and Y.L. designed the experiments. All authors participated in the interpretation of the data and the production of the final manuscript.

References

[1] T.R. Geiger, D.S. Peeper, Metastasis mechanisms, Biochim. Biophys. Acta. Rev. Cancer, 1796 (2009) 293-308.

[2] Z. Chen, Y. Chen, M. Xu, L. Chen, X. Zhang, K.K. To, H. Zhao, F. Wang, Z. Xia, X. Chen, L. Fu,

Osimertinib (AZD9291) Enhanced the efficacy of chemotherapeutic agents in ABCB1- and ABCG2-overexpressing cells in vitro, in vivo, and ex vivo, Mol. Cancer. Ther, 15 (2016) 1845-1858.

[3] Y.W. Bahk, On launching a new twenty-first century quarterly journal, nuclear medicine and molecular imaging, Nucl. Med. Mol. Imaging, 44 (2010) 1-2.

[4] S. Li, Y. Chen, Y. Zhang, X. Jiang, Y. Jiang, X. Qin, H. Yang, C. Wu, Y. Liu, Shear stress promotes anoikis resistance of cancer cells via caveolin-1-dependent extrinsic and intrinsic apoptotic pathways, J. Cell. Physiol, (2019) 3730-3743.

[5] S. Li, N.Y. Xiong, Y.T. Peng, K. Tang, H.X. Bai, X.Y. Lv, Y. Jiang, X. Qin, H. Yang, C.H. Wu, P. Zhou, Y.Y. Liu, Acidic pHe regulates cytoskeletal dynamics through conformational integrin beta 1 activation and promotes membrane protrusion, Biochim. Biophys. Acta. Mol. Basis. Dis, 1864 (2018) 2395-2408.

[6] J. Zhang, L. Li, Y. Peng, Y. Chen, X. Lv, S. Li, X. Qin, H. Yang, C. Wu, Y. Liu, Surface chemistry induces mitochondria-mediated apoptosis of breast cancer cells via PTEN/PI3K/AKT signaling pathway, Biochim. Biophys. Acta. Mol.Cell. Res, 1865 (2018) 172-185.

[7] X. Qin, J. Li, J. Sun, L. Liu, D. Chen, Y. Liu, Low shear stress induces ERK nuclear localization and YAP activation to control the proliferation of breast cancer cells, Biochem. Biophys. Res. Commun, 510 (2019) 219-223.

[8] J.I. Lopez, I. Kang, W.K. You, D.M. McDonald, V.M. Weaver, In situ force mapping of mammary gland transformation, Integr. Biol (Camb), 3 (2011) 910-921.

[9] P. Lu, V.M. Weaver, Z. Werb, The extracellular matrix: a dynamic niche in cancer progression, J. Cell. Biol, 196 (2012) 395-406.

[10] X. Qin, B.O. Park, J. Liu, B. Chen, V. Choesmel-Cadamuro, K. Belguise, W.D. Heo, X. Wang, Cell-matrix adhesion and cell-cell adhesion differentially control basal myosin oscillation and Drosophila egg chamber elongation, Nat. Commun, 8 (2017) 14708.

[11] X. Qin, E. Hannezo, T. Mangeat, C. Liu, P. Majumder, J.Y. Liu, V. Choesmel-Cadamuro, J.A. McDonald, Y.Y. Liu, B. Yi, X.B. Wang, A biochemical network controlling basal myosin oscillation, Nat. Commun, 9 (2018) 1210.

[12] R. Ross, Atherosclerosis--an inflammatory disease, N. Engl. J. Med, 340 (1999) 115-126.

[13] T.J. Liu, B.C. Sun, X.L. Zhao, X.M. Zhao, T. Sun, Q. Gu, Z. Yao, X.Y. Dong, N. Zhao, N. Liu, CD133+ cells with cancer stem cell characteristics associates with vasculogenic mimicry in triple-negative breast cancer, Oncogene, 32 (2013) 544-553.

[14] X. Yang, S.K. Sarvestani, S. Moeinzadeh, X. He, E. Jabbari, Three-dimensional-engineered matrix to study cancer stem cells and tumorsphere formation: effect of matrix modulus, Tissue. Eng. Part. A, 19 (2013) 669-684.

[15] X. Tang, T.B. Kuhlenschmidt, J. Zhou, P. Bell, F. Wang, M.S. Kuhlenschmidt, T.A. Saif, Mechanical force affects expression of an in vitro metastasis-like phenotype in HCT-8 cells, Biophys. J, 99 (2010) 2460-2469.

[16] G. Schlunck, H. Han, T. Wecker, D. Kampik, T. Meyer-ter-Vehn, F. Grehn, Substrate rigidity modulates cell matrix interactions and protein expression in human trabecular meshwork cells, Invest. Ophthalmol. Vis. Sci, 49 (2008) 262-269.

[17] E. Jabbari, S.K. Sarvestani, L. Daneshian, S. Moeinzadeh, Optimum 3D Matrix Stiffness for Maintenance of Cancer Stem Cells Is Dependent on Tissue Origin of Cancer Cells, PLoS. One, 10 (2015) e0132377.

[18] S. Dedhar, B. Williams, G. Hannigan, Integrin-linked kinase (ILK): a regulator of integrin and growth-factor signalling, Trends. Cell. Biol, 9 (1999) 319-323.

[19] S. Shishido, H. Bonig, Y.M. Kim, Role of integrin alpha4 in drug resistance of leukemia, Front. Oncol, 4 (2014) 99.

[20] N. Elad, T. Volberg, I. Patla, V. Hirschfeld-Warneken, C. Grashoff, J.P. Spatz, R. Fassler, B. Geiger, O. Medalia, The role of integrin-linked kinase in the molecular architecture of focal adhesions, J. Cell. Sci, 126 (2013) 4099-4107.

[21] C. Hausmann, A. Temme, N. Cordes, I. Eke, ILKAP, ILK and PINCH1 control cell survival of p53-wildtype glioblastoma cells after irradiation, Oncotarget, 6 (2015) 34592-34605.

[22] F. Zanconato, M. Forcato, G. Battilana, L. Azzolin, E. Quaranta, B. Bodega, A. Rosato, S. Bicciato, M. Cordenonsi, S. Piccolo, Genome-wide association between YAP/TAZ/TEAD and AP-1 at enhancers drives oncogenic growth, Nat. Cell. Biol, 17 (2015) 1218-1227.

[23] M.H. Kim, J. Kim, H. Hong, S.H. Lee, J.K. Lee, E. Jung, J. Kim, Actin remodeling confers BRAF inhibitor resistance to melanoma cells through YAP/TAZ activation, EMBO. J, 35 (2016) 462-478.

[24] C.H. Lin, F.A. Pelissier, H. Zhang, J. Lakins, V.M. Weaver, C. Park, M.A. LaBarge, Microenvironment rigidity modulates responses to the HER2 receptor tyrosine kinase inhibitor lapatinib via YAP and TAZ transcription factors, Mol. Biol. Cell, 26 (2015) 3946-3953.

[25] O. Tredan, C.M. Galmarini, K. Patel, I.F. Tannock, Drug resistance and the solid tumor microenvironment, J. Natl. Cancer. Inst, 99 (2007) 1441-1454.

[26] P.A. Netti, D.A. Berk, M.A. Swartz, A.J. Grodzinsky, R.K. Jain, Role of extracellular matrix assembly in interstitial transport in solid tumors, Cancer. Res, 60 (2000) 2497-2503.

[27] H. Denys, G. Braems, K. Lambein, P. Pauwels, A. Hendrix, A. De Boeck, V. Mathieu, M. Bracke, O. De Wever, The extracellular matrix regulates cancer progression and therapy response: implications for prognosis and treatment, Curr. Pharm. Des, 15 (2009) 1373-1384.

[28] Y. Peng, Z.Y. Chen, Y. Chen, S. Li, Y. Jiang, H. Yang, C.H. Wu, F.M. You, C. Zheng, J. Zhu, Y. Tan, X. Qin, Y.Y. Liu, ROCK isoforms differentially modulate cancer cell motility by mechanosensing substrate stiffness, Acta. Biomater, 88 (2019) 86-101.

[29] M.D. Jacobson, M. Weil, M.C. Raff, Programmed cell death in animal development, Cell, 88 (1997) 347-354.

[30] J. Kwon, K.Y. Eom, T.R. Koo, B.H. Kim, E. Kang, S.W. Kim, Y.J. Kim, S.Y. Park, I.A. Kim, A Prognostic Model for Patients with Triple-Negative Breast Cancer: Importance of the Modified Nottingham Prognostic Index and Age, J. Breast. Cancer, 20 (2017) 65-73.

[31] G. Housman, S. Byler, S. Heerboth, K. Lapinska, M. Longacre, N. Snyder, S. Sarkar, Drug resistance in cancer: an overview, Cancers (Basel), 6 (2014) 1769-1792.

[32] S.L. Lee, E.C. Hsu, C.C. Chou, H.C. Chuang, L.Y. Bai, S.K. Kulp, C.S. Chen, Identification and characterization of a novel integrin-linked kinase inhibitor, J. Med. Chem, 54 (2011) 6364-6374.

[33] M.A. Wozniak, R. Desai, P.A. Solski, C.J. Der, P.J. Keely, ROCK-generated contractility regulates breast epithelial cell differentiation in response to the physical properties of a three-dimensional collagen matrix, J. Cell. Biol, 163 (2003) 583-595.

[34] E. Tzima, M.A. del Pozo, S.J. Shattil, S. Chien, M.A. Schwartz, Activation of integrins in

endothelial cells by fluid shear stress mediates Rho-dependent cytoskeletal alignment, EMBO. J, 20 (2001) 4639-4647.

[35] M.F. Pang, M.J. Siedlik, S. Han, M. Stallings-Mann, D.C. Radisky, C.M. Nelson, Tissue Stiffness and Hypoxia Modulate the Integrin-Linked Kinase ILK to Control Breast Cancer Stem-like Cells, Cancer. Res, 76 (2016) 5277-5287.

[36] M. Fischer, P. Rikeit, P. Knaus, C. Coirault, YAP-Mediated Mechanotransduction in Skeletal Muscle, Front. Physiol, 7 (2016) 41.

[37] Z. Jia, Role of integrin-linked kinase in drug resistance of lung cancer, Onco. Targets. Ther, 8 (2015) 1561-1565.

[38] J.Y. Lee, J.K. Chang, A.A. Dominguez, H.P. Lee, S. Nam, J. Chang, S. Varma, L.S. Qi, R.B. West, O. Chaudhuri, YAP-independent mechanotransduction drives breast cancer progression, Nat. Commun, 10 (2019) 1848.

[39] J. Solon, I. Levental, K. Sengupta, P.C. Georges, P.A. Janmey, Fibroblast adaptation and stiffness matching to soft elastic substrates, Biophys. J, 93 (2007) 4453-4461.

[40] T. Yeung, P.C. Georges, L.A. Flanagan, B. Marg, M. Ortiz, M. Funaki, N. Zahir, W. Ming, V. Weaver, P.A. Janmey, Effects of substrate stiffness on cell morphology, cytoskeletal structure, and adhesion, Cell. Motil. Cytoskeleton, 60 (2005) 24-34.

[41] J.Y. Wong, A. Velasco, P. Rajagopalan, Q. Pham, Directed movement of vascular smooth muscle cells on gradient-compliant hydrogels, Langmuir, 19 (2003) 1908-1913.

[42] A. Zemel, F. Rehfeldt, A.E.X. Brown, D.E. Discher, S.A. Safran, Optimal matrix rigidity for stress-fibre polarization in stem cells, Nat. Phys, 6 (2010) 468-473.

[43] M.W. Conklin, P.J. Keely, Why the stroma matters in breast cancer Insights into breast cancer patient outcomes through the examination of stromal biomarkers, Cell. Adh. Migr, 6 (2012) 249-260.

Figure Legends

Fig.1. Intermediate Stiffness matrix promoted cell proliferation and inhibited cell death. (**A**) MDA-MB-231 cells were cultured on polyacrylamide hydrogels with different stiffness for 24 h, and then treated with different concentrations of doxorubicin (Dox) for 48 h. The different PAA gel substrates were defined as low (10 kPa), intermediate (38 kPa) and high (57 kPa) rigidities respectively. Cell viability was detected by CCK-8, 3 mg/L doxorubicin was selected for further study, because the cell survival rates were higher than 70% in all substrates. (**B**) Cells were treated with 3 mg/L of doxorubicin for 48 h. The expression of Ki67 was detected by immunofluorescence, in which blue indicates the nucleus stained by DAPI and green indicates Ki67. The scale was 50 μm. (**C**) The proportion of Ki67-positive cells on different stiffness was analyzed. (**D**) Cells were digested, stained with Calcein-AM and PI. Green is living cells and red is cells that have undergone apoptosis or necrosis. Scale bar=100 μm. (**E**) Three images were randomly selected for each stiffness. Image J was used for quantitative analysis of red and green fluorescence. The red fluorescence intensity was compared with the total fluorescence intensity. (**F**) The expression of apoptosis-related proteins was detected by Western blot. (**G**) Relative expression of C-caspase3/Caspase3, Bcl-2/Bax, C-PARP/PARP. *p<0.05, **p<0.005, ***p<0.0005.

Fig.2. Intermediate stiffness matrix decreased doxorubicin uptake and increased resistance in breast cancer cells. (**A**) Confocal microscopy was used to detect the accumulation of doxorubicin in the cells. Blue is the nucleus and red is doxorubicin. Scale bar is 20 μm. (**B**) Flow cytometry was used to test the uptake of doxorubicin by cells. (**C**) The flow cytometry results of relative doxorubicin fluorescence intensity were analyzed. (**D**) MDA-MB-231

cells with different stiffness were treated with 10 μM P-gp fluorescent substrate rhodamine solution (Rho123) for 1 h. Cells incubated in medium containing Elacridar (2 μM), a P-gp inhibitor, were used as positive control, and the fluorescence intensity was measured by flow cytometry. (**E, F**) *q*PCR (E) and Western blot (F) detected P-gp expression at different stiffness. *p<0.05, **p<0.005.

Fig.3. Intermediate rigidity promoted ILK expressions. (**A**) mRNA levels of ILK in normal breast and breast carcinoma tissues (left panel), breast carcinoma in different stages (right panel) were analyzed, patient data were from the Oncomine public sample database, sample: Curtis Breast, Grouped by Cancer Type; TCGA Breast Grouped by Stage (Invasive Ductal Breast Carcinoma). (**B**) Kaplan-Meier analysis of mortality differences in patients with high (blue line) and low ILK expressions (red line). The data was from R_2 microarray public sample database. Sample: Tumor Breast (MDC)-Bertucci-266MAS5.0-u133p2, *p=0.045. (**C**) The mRNA expression of ILK in MDA-MB-231 and MDA-MB-468 cells at different stiffness. (**D**) ILK protein expression at different stiffness in MDA-MB-231 and MDA-MB-468 cells. (**E**) Image J performed a grey scale analysis of the (D) results. *p<0.05, **p<0.005.

Fig.4. Intermediate rigidity induced YAP-mediated P-gp expressions. (**A**) Kaplan-Meier analysis of mortality in patients with high (blue line) and low ILK expression (red line). The data was from R_2 microarray public sample database, sample: Tumor Breast Taxane Anthracycline Booser 508MAS5.0-u133a, *p=0.01. **(B, C)** The expression of YAP and upstream related proteins in MDA-MB-231 cells at different stiffness were analyzed. **(D)** Luciferase reporter assay detected YAP transcriptional activity. **(E)** *q*PCR detected YAP target gene expression on different stiffness. **(F)** P-gp mRNA

levels were detected by *q*PCR in the inhibition of YAP and ILK. *p<0.05, **p<0.005, ***p<0.0005.

Fig.5. ILK controlled YAP activation and nuclear translocation. (**A**) Correlation between YAP and ILK in normal breast (left) and breast carcinoma tissues (right) were analyzed. Patient data was derived from the Oncomine public sample database, sample: Curtis Breast, Grouped by Cancer Type. (**B**) Cells at 38 kPa were treated with different concentrations of T315 and immunofluorescence was used to detect the entry of YAP into the nucleus. (**C**) Image J analyzed the fluorescence intensity of YAP in the nucleus and cytoplasm. The fluorescence intensity of the cytoplasm which was smaller than that of the nucleus, equal to the nucleus, larger than the nucleus were quantified. (**D**) The cells at 38 kPa were treated with different concentrations of T315. Western blot was used to detect the expression of YAP and its related molecules.

Fig.6. Intermediate rigidity induced YAP expression and activity. (**A**) Immunofluorescence of YAP nuclear localization on different stiffness. Scale bar is 20 μm. **(B)** Image J analyzed the fluorescence intensity of YAP in the nucleus and cytoplasm. The fluorescence intensity of the cytoplasm which was smaller than that of the nucleus, equal to the nucleus, larger than the nucleus were quantified. (**C**) Extract the cytoplasmic and nuclear proteins of MDA-MB-231 cells from different stiffness, the expression of YAP and p-YAP in cytoplasm and nucleus were detected.

Fig.7. Matrix stiffness regulates cell doxorubicin resistance by ILK-mediated YAP activation. (**A**) Schematic cartoon to summarize the process of ILK mediated YAP activation in stiff matrix substrate. ILK promotes drug resistance through inactivation of Merlin/MST/LATS, the key component

of the hippo pathway. The inactivation of Merlin/MST/LATS results in the YAP nuclear translocation and promotes the resistance of drugs. (**B**) Schematic cartoon to summarize the poor doxorubicin resistance in low and high stiffness matrix substrates. Decreased ILK kinase activity de-phosphorylated Merlin and phosphorylated MST and LATS, leading to the activation of Merlin/MST/LATS, thus phosphorylated YAP, which hindered its nuclear translocation.

Highlights

- High expressions of ILK and YAP reduce the survival rates of breast cancer patients
- ILK and YAP inhibition results in lower levels of cell drug resistance
- Drug resistance is closely associated with the inactivation of the hippo pathway of Merlin/MST/LATS
- Matrix stiffness regulates the drug resistance of breast cancer cells through ILK-mediated YAP activation

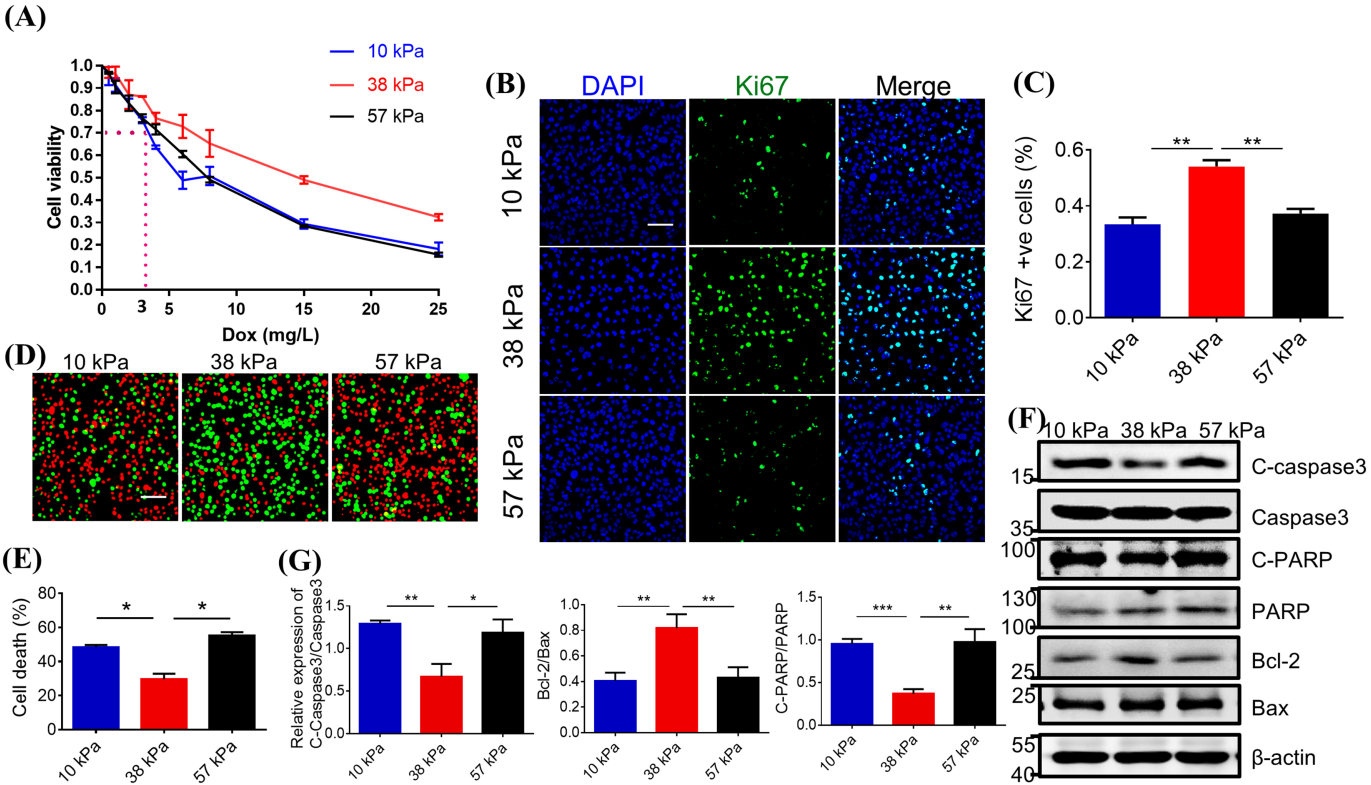
(A)
10 kPa
38 kPa
57 kPa
Cell viability
Dox (mg/L)
(B)
DAPI
Ki67
Merge
10 kPa
38 kPa
57 kPa
(C)
Ki67 +ve cells (%)
(D)
10 kPa
38 kPa
57 kPa
(E)
Cell death (%)
(F)
10 kPa 38 kPa 57 kPa
C-caspase3
Caspase3
C-PARP
PARP
Bcl-2
Bax
β-actin
(G)
Relative expression of C-Caspase3/Caspase3
Bcl-2/Bax
C-PARP/PARP

Figure 1

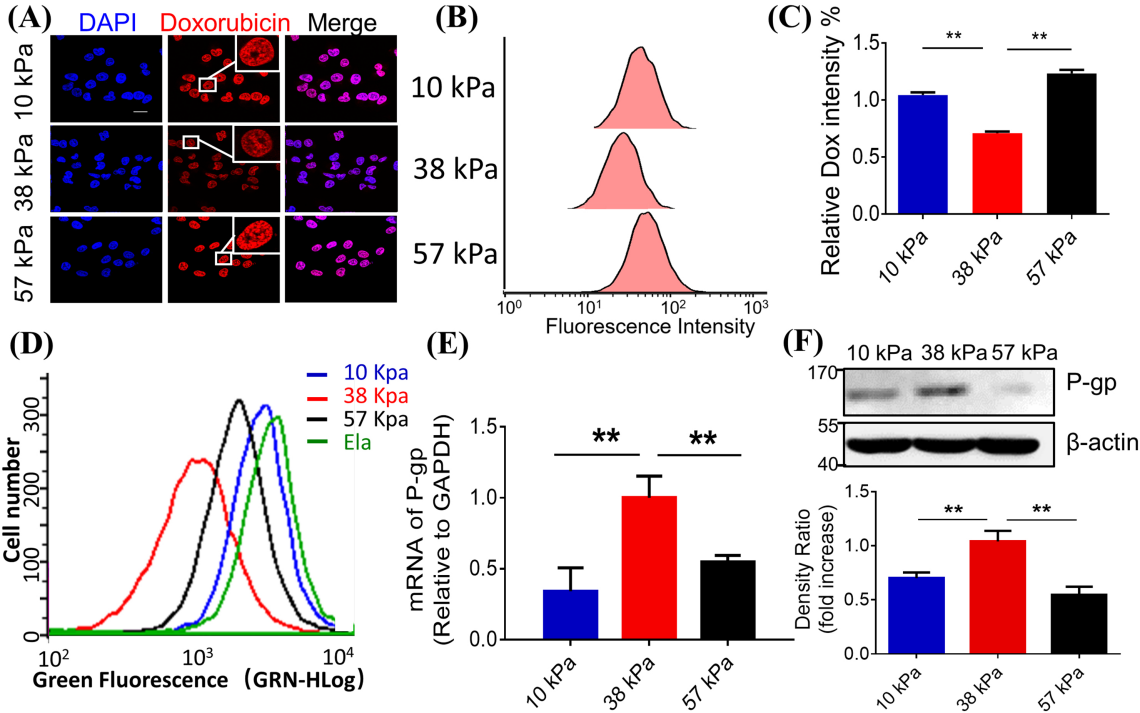
(A)
DAPI
Doxorubicin
Merge
10 kPa
38 kPa
57 kPa
(B)
10 kPa
38 kPa
57 kPa
Fluorescence Intensity
(C)
Relative Dox intensity %
**
**
10 kPa
38 kPa
57 kPa
(D)
10 Kpa
38 Kpa
57 Kpa
Ela
Cell number
Green Fluorescence (GRN-HLog)
(E)
mRNA of P-gp
(Relative to GAPDH)
**
**
10 kPa
38 kPa
57 kPa
(F)
10 kPa 38 kPa 57 kPa
P-gp
β-actin
Density Ratio
(fold increase)
**
**
10 kPa
38 kPa
57 kPa

Figure 2

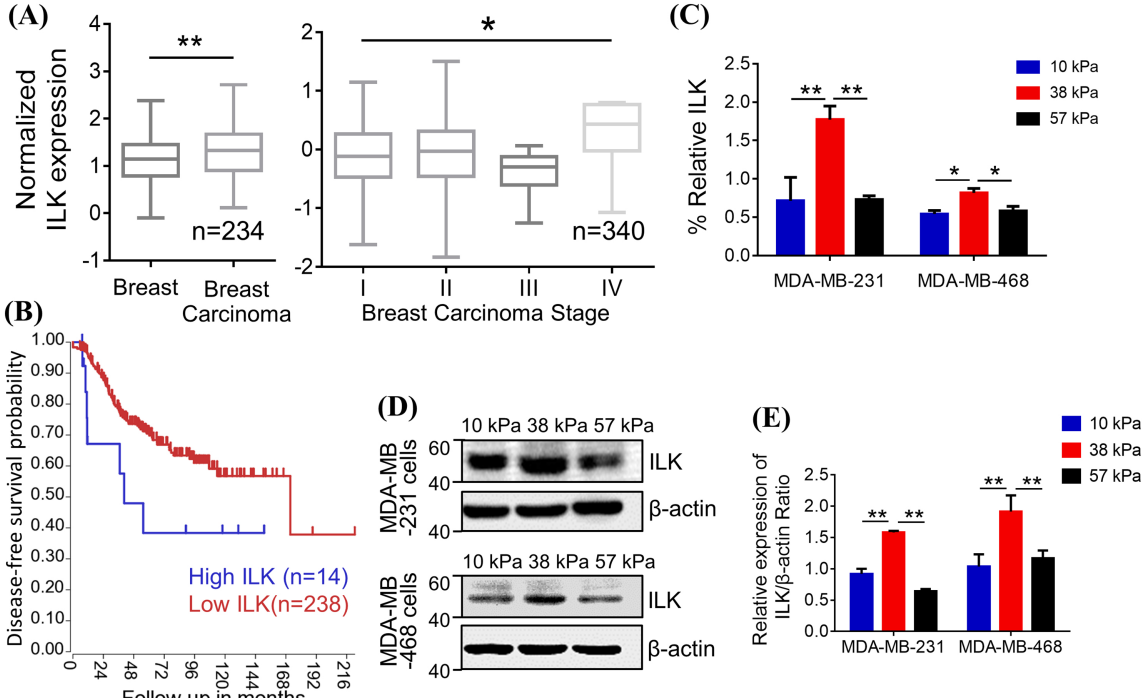
(A)
Normalized ILK expression
**
n=234
Breast
Breast Carcinoma
*
n=340
I
II
III
IV
Breast Carcinoma Stage
(B)
Disease-free survival probability
High ILK (n=14)
Low ILK(n=238)
Follow up in months
(C)
% Relative ILK
10 kPa
38 kPa
57 kPa
MDA-MB-231
MDA-MB-468
(D)
10 kPa 38 kPa 57 kPa
MDA-MB -231 cells
ILK
β-actin
MDA-MB -468 cells
(E)
Relative expression of ILK/β-actin Ratio
MDA-MB-231
MDA-MB-468

Figure 3

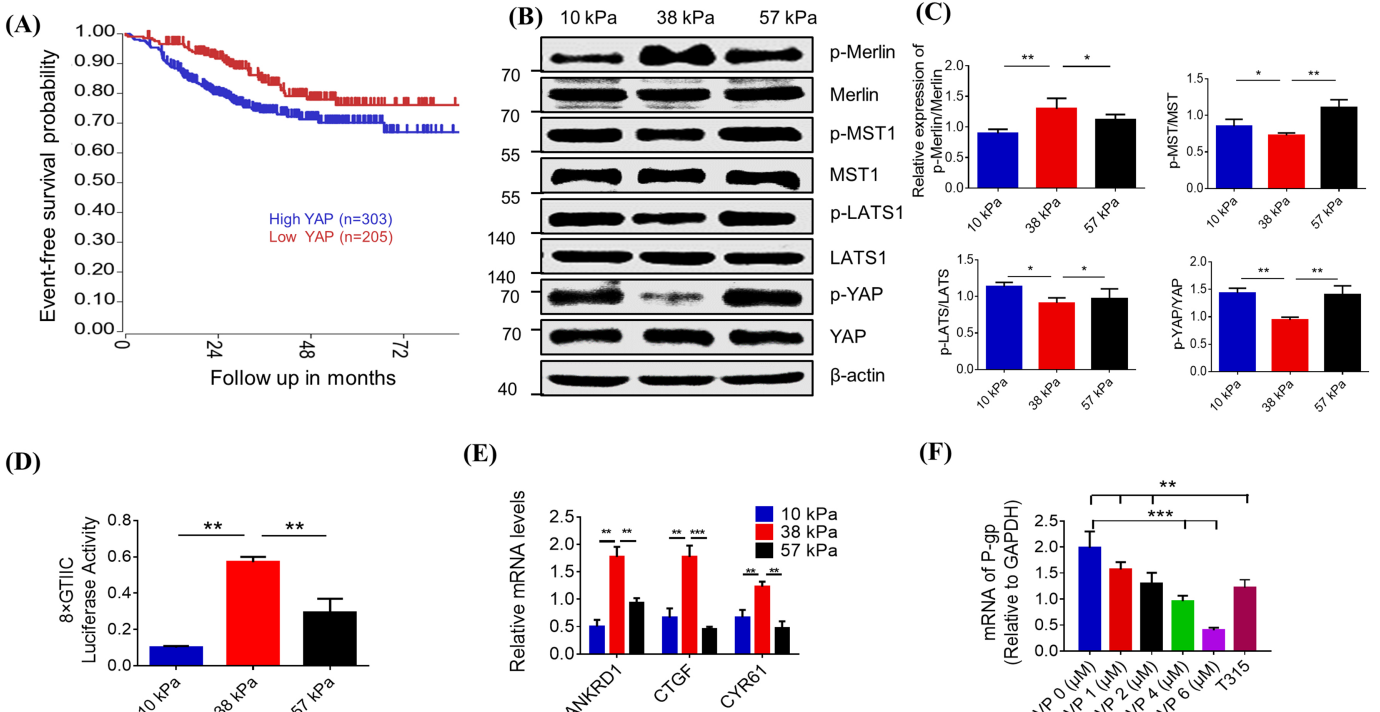
(A)
Event-free survival probability
1.00
0.90
0.80
0.70
0.60
0.50
0.40
0.30
0.20
0.10
0.00
0
24
48
72
Follow up in months
High YAP (n=303)
Low YAP (n=205)
(B)
10 kPa
38 kPa
57 kPa
p-Merlin
Merlin
p-MST1
MST1
p-LATS1
LATS1
p-YAP
YAP
β-actin
70
70
55
55
140
140
70
70
40
(C)
Relative expression of p-Merlin/Merlin
p-MST/MST
p-LATS/LATS
p-YAP/YAP
10 kPa
38 kPa
57 kPa
(D)
8×GTIIC Luciferase Activity
(E)
Relative mRNA levels
10 kPa
38 kPa
57 kPa
ANKRD1
CTGF
CYR61
(F)
mRNA of P-gp (Relative to GAPDH)
VP 0 (μM)
VP 1 (μM)
VP 2 (μM)
VP 4 (μM)
VP 6 (μM)
T315

Figure 4

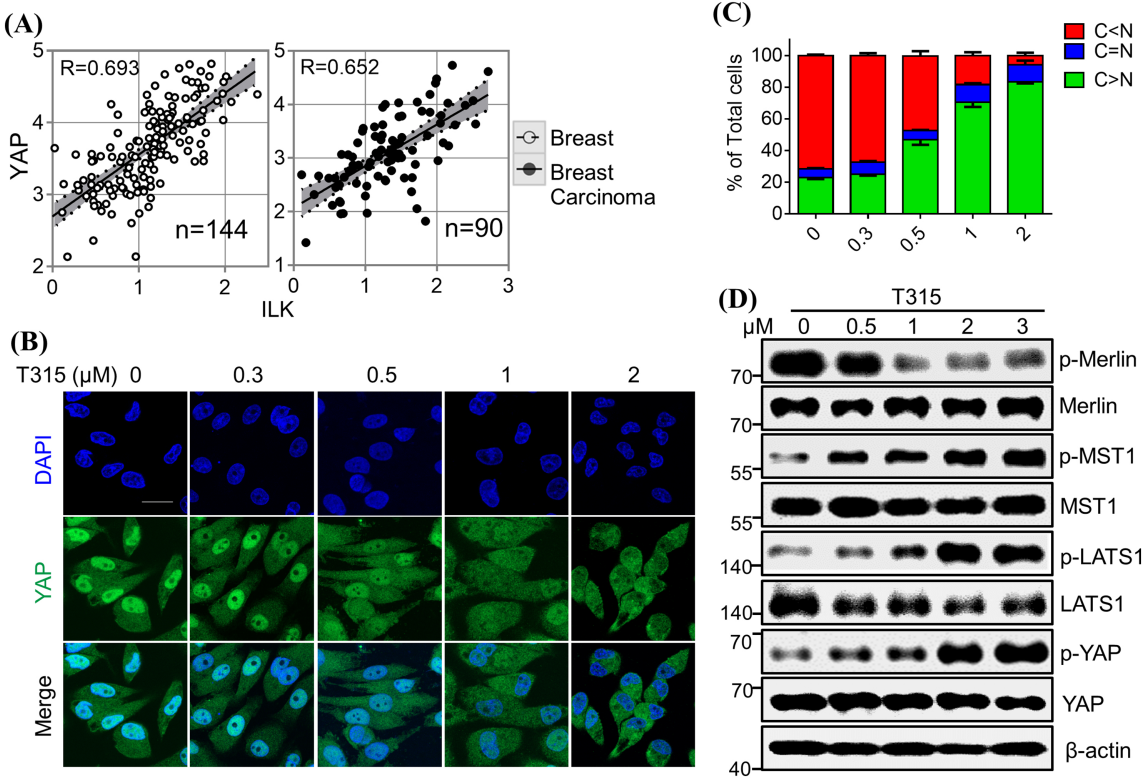
(A)
R=0.693
n=144
R=0.652
n=90
YAP
ILK
Breast
Breast Carcinoma
(B)
T315 (μM) 0 0.3 0.5 1 2
DAPI
YAP
Merge
(C)
% of Total cells
C<N
C=N
C>N
0 0.3 0.5 1 2
(D)
T315
μM 0 0.5 1 2 3
p-Merlin
Merlin
p-MST1
MST1
p-LATS1
LATS1
p-YAP
YAP
β-actin

Figure 5

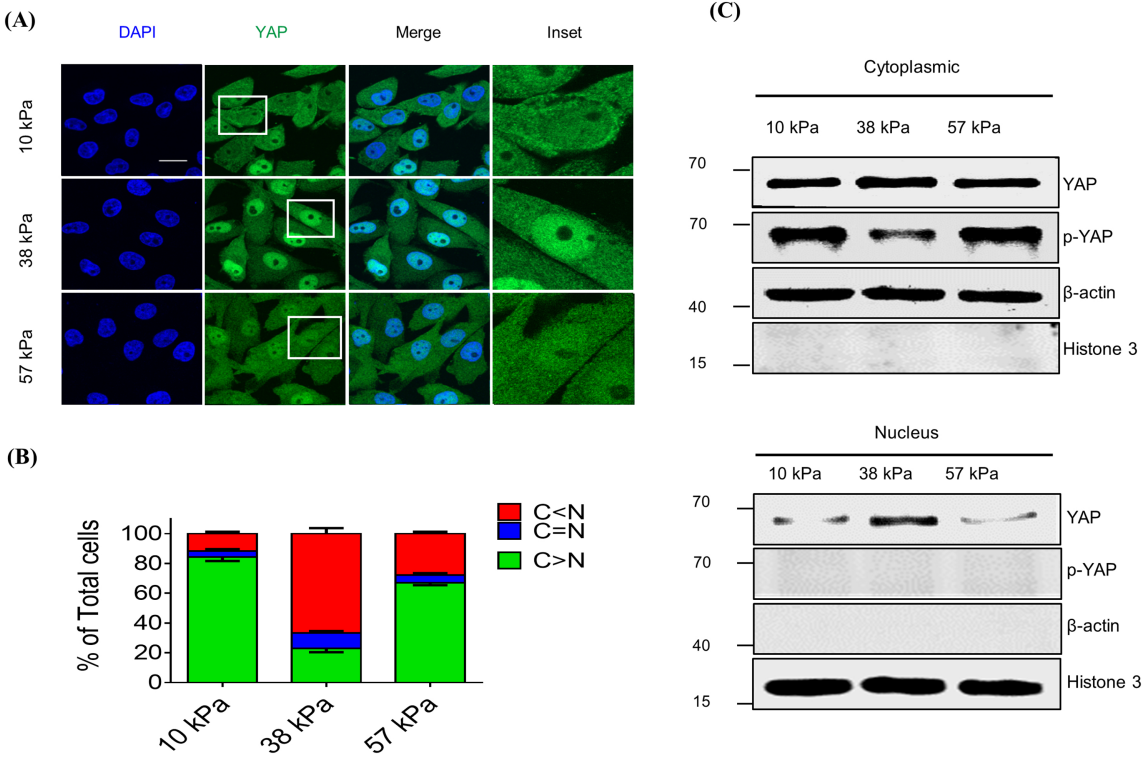
(A)
DAPI
YAP
Merge
Inset
10 kPa
38 kPa
57 kPa
(B)
% of Total cells
100
80
60
40
20
0
C<N
C=N
C>N
10 kPa
38 kPa
57 kPa
(C)
Cytoplasmic
10 kPa
38 kPa
57 kPa
70
70
40
15
YAP
p-YAP
β-actin
Histone 3
Nucleus
10 kPa
38 kPa
57 kPa
70
70
40
15
YAP
p-YAP
β-actin
Histone 3

Figure 6

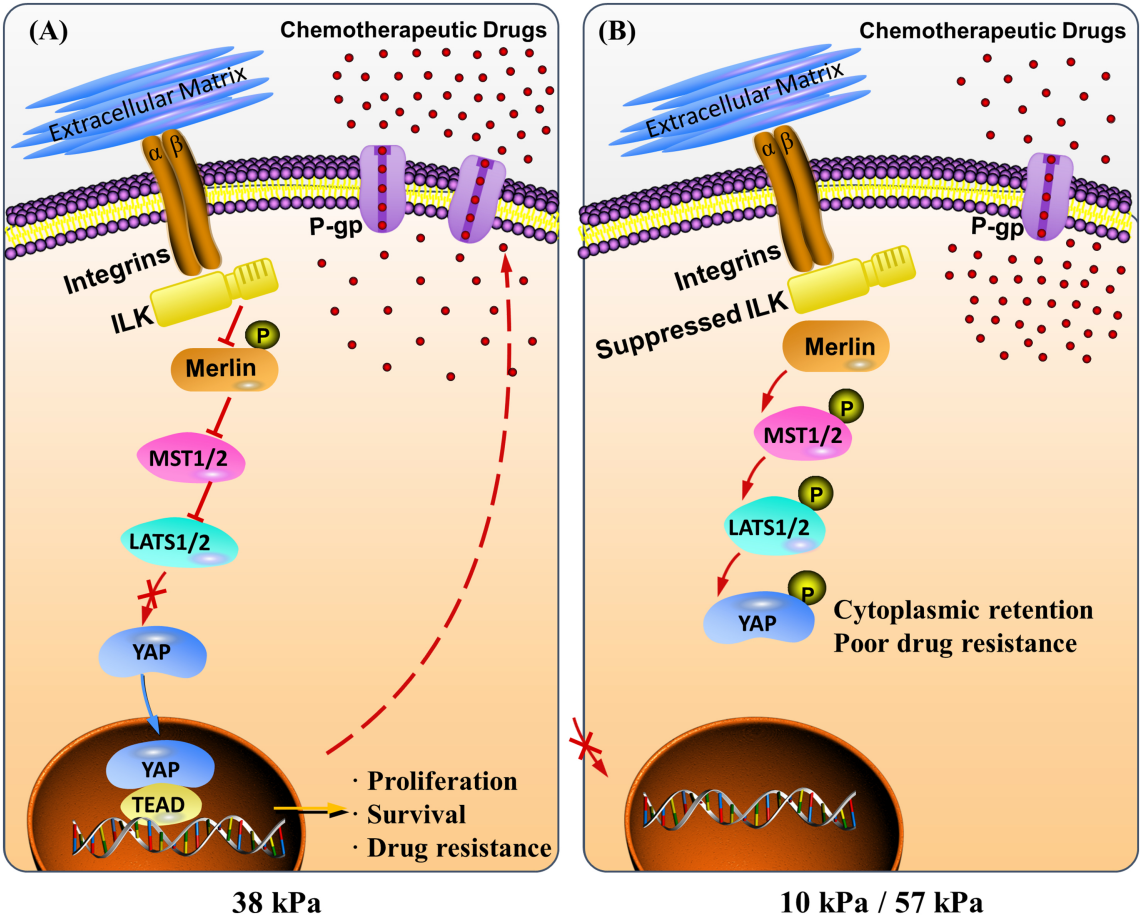
(A)
Chemotherapeutic Drugs
Extracellular Matrix
α
β
Integrins
P-gp
ILK
P
Merlin
MST1/2
LATS1/2
YAP
YAP
TEAD
· Proliferation
· Survival
· Drug resistance
38 kPa
(B)
Chemotherapeutic Drugs
Extracellular Matrix
α
β
Integrins
P-gp
Suppressed ILK
Merlin
P
MST1/2
P
LATS1/2
P
YAP
Cytoplasmic retention
Poor drug resistance
10 kPa / 57 kPa

Figure 7